

## RATE-SENSITIVITY AND SHORT TERM RELAXATION BEHAVIOR OF AISI TYPE 304 STAINLESS STEEL AT ROOM TEMPERATURE AND AT 650 °C; INFLUENCE OF PRIOR AGING.

Marina B. Ruggles\*  
Engineering Technology Division  
Oak Ridge National Laboratory\*\*  
Oak Ridge, Tennessee 37831-8051

CONF-890721--9

DE89 007823

and

Erhard Krempl  
Mechanics of Materials Laboratory  
Rensselaer Polytechnic Institute  
Troy, NY 12180-3590

### ABSTRACT

The strain rate sensitivity and short term relaxation behavior of Type 304 Stainless Steel were investigated in the uniaxial strain rate jump tests with intermittent periods of relaxation at room temperature and at 650 °C. At room temperature material exhibited conventional strain rate sensitivity and no strain rate history effect. The high-temperature experimental results revealed a complex and dramatically different material behavior. At 650 °C the pattern of strain rate sensitivity was not set as soon as the plastic flow was fully established, but continued to evolve with the further straining in the plastic range. Test results indicate that at 650 °C the material may exhibit a strain rate history effect. Both at room temperature and at 650 °C the relaxation behavior was independent of the stress and/or strain level at the beginning of the relaxation, but depended nonlinearly on the strain rate preceding the relaxation test. Prior aging had no significant influence on the rate-dependent material response. The irregular material behavior at 650 °C is attributed to dynamic strain aging as indicated by serrated stress-strain curves (the Portevin-LeChatelier effect).

### INTRODUCTION

The service life prediction of structural components used at elevated temperatures requires that the inelastic stress-strain

---

\* Formerly at Rensselaer Polytechnic Institute.

\*\*Operated by Martin Marietta Energy Systems, Inc., under contract DE-AC05-84OR21400 with the U.S. Department of Energy.

# MASTER

## **DISCLAIMER**

**This report was prepared as an account of work sponsored by an agency of the United States Government. Neither the United States Government nor any agency thereof, nor any of their employees, makes any warranty, express or implied, or assumes any legal liability or responsibility for the accuracy, completeness, or usefulness of any information, apparatus, product, or process disclosed, or represents that its use would not infringe privately owned rights. Reference herein to any specific commercial product, process, or service by trade name, trademark, manufacturer, or otherwise does not necessarily constitute or imply its endorsement, recommendation, or favoring by the United States Government or any agency thereof. The views and opinions of authors expressed herein do not necessarily state or reflect those of the United States Government or any agency thereof.**

---

## **DISCLAIMER**

**Portions of this document may be illegible in electronic image products. Images are produced from the best available original document.**

response under the operating conditions be evaluated. A very complex deformation behavior of metallic materials at high temperatures has been observed earlier [1, 2]. Goodall et al [3] and Clement et al [4] considered behavior of austenitic stainless steel under cyclic loading at elevated temperature. Inelastic behavior of high temperature materials under biaxial stress state was examined by Inoue et al [5]. Nonlinear material behavior at elevated temperature is further complicated by the presence of the Portevin-LeChatelier (PLC) effect [6-11] and dynamic strain aging [12-15].

Recently a number of researchers [16-19] studied room temperature strain rate sensitivity, short term relaxation and cyclic hardening properties of engineering alloys. In the present work these properties are investigated for type 304 austenitic stainless steel at room temperature and at 650 °C. Results reveal dramatic differences in the strain rate sensitivity patterns at room and elevated temperatures. In this case testing is of an exploratory nature, experimental observations may serve as guidelines for constitutive modeling. The influence of prior aging on the rate dependent material behavior at room temperature and at 650 °C is also considered.

Servocontrolled mechanical testing with computer control is used for experiments. Servocontrolled testing permits accurate control of the loading rate, and is therefore well suited for the current program.

## TESTING EQUIPMENT

The material tested was AISI Type 304 austenitic stainless steel with the following chemical composition : 0.044% C; 1.26% Mn; 0.033% P; 0.016% S; 0.45% Si; 9.5% Ni; 18.64% Cr; 0.34% Mo; 0.25% Cu; reference heat 9T-2796. Test specimens were similar to those shown in Fig. 1 of [17]. Prior to testing machined specimens were annealed in vacuum at 1093 °C for 90 minutes. After annealing specimens were subjected to the following aging heat treatment:

- a). Solution heat treatment in vacuum: 20 min at 1,050 °C.
- b). Water quench.
- c). Precipitation treatment:  
200 h at 650 °C - group C;  
2000 h at 650 °C - group D.

To avoid oxidation during the precipitation treatment, each specimen was encapsulated in an evacuated quartz tube together with the strip of Tantalum foil. Unaged specimens, i. e. specimens subjected

to annealing only, were also included in the experimental program as reference.

A servocontrolled MTS axial-torsion testing machine together with the MTS 463 Data/Control processor were used for computerized testing and data acquisition, which was accomplished by a program in MTS Basic. The load (engineering stress), displacement (engineering strain), and the command signal (strain) were measured and recorded; the digitized test data were stored on floppy disks. The data acquisition intervals were established on the basis of stress, i. e. a data point was recorded whenever the stress changed by 2.9 MPa. After the test the digitized data can be recalled for processing and interpretation. The entire history is available for analysis. During the tests load and displacement were also plotted on an XY recorder.

Displacement in the gage section was measured with an MTS clip-on extensometer during the room temperature tests, and with an MTS high-temperature uniaxial extensometer during the elevated temperature tests. In high-temperature tests an MTS clamshell furnace was used to heat the specimens and maintain the elevated temperature during the test. Three thermocouples were placed on the gage section of the specimen. For the duration of the tests the temperature in the gage section remained reasonably uniform, and stayed within  $\pm 3$  °C of the nominal temperature. In very rare instances variations of  $\pm 5$  °C were encountered.

## TESTING PROGRAM

A strain controlled Strain Rate Jump Test (SRJT), which is schematically shown in Fig. 1a, constituted the major part of history I. The SRJT consists of alternating periods of monotonic loading and relaxation. Segments of monotonic loading are characterized by a different strain rate each. In test history I the SRJT (distance OJ in Fig. 1a) was repeated 8 times, so that the specimen reached a total strain of about 52%. Test history I was performed both at room temperature and at 650 °C.

As the response of the unaged material to history I at 650 °C was rather unexpected, two more test histories were introduced. Test history II is based on a SRJT in which all periods of relaxation (AB, CD, EF, GH in Fig. 1a) are omitted; this modification, called SRJT-1 (see Fig. 1b), contains only the strain rate changes. In history II SRJT-1 is repeated 8 times or until failure. In test history III modification SRJT-2 (shown in Fig. 1c) was introduced, in order to determine whether the material behavior during monotonic

loading with the "fast" strain rates of  $1.5 \times 10^{-3} \text{ s}^{-1}$  and  $1.5 \times 10^{-4} \text{ s}^{-1}$  in history I (DE and HI in Fig. 1a) was in any way influenced by the "slow" strain rate segments in the SRJT. In SRJT-2 monotonic loading with the "slow" strain rates of  $1.5 \times 10^{-5} \text{ s}^{-1}$  and  $1.5 \times 10^{-6} \text{ s}^{-1}$  (BC and FG in Fig. 1a) and the preceding relaxation tests (AB and EF in Fig. 1a) were omitted. SRJT-2 was repeated 8 times or until failure. Test histories II and III were restricted to 650 °C.

To provide a better understanding of the rate-sensitivity of the material at 650 °C, two constant strain rate tensile tests were performed for  $\dot{\epsilon} = 1.5 \times 10^{-3} \text{ s}^{-1}$  and  $\dot{\epsilon} = 1.5 \times 10^{-5} \text{ s}^{-1}$ . Both of these tests were in fact successions of experiments, each covering a 15% strain interval (the extensometer range limit). Thus each of the constant strain rate tests was interrupted at  $\epsilon = 15\%$  and  $\epsilon = 30\%$  (for  $\dot{\epsilon} = 1.5 \times 10^{-5} \text{ s}^{-1}$ ), where the extensometer was rezeroed. It should be also noted, that due to the range limitations the extensometer had to be readjusted between the individual strain rate jump tests. In general no cool down took place between the SRJTs, and the time required for readjustment was negligible compared to the total SRJT time. In some instances, however, cool down was necessary. In case of specimen 8, the cool down took place between SRJTs #3 and 4, and SRJTs #6 and 7. For specimen 9 the cool down occurred between SRJTs #4 and 5.

Due to the shortage of specimens, test histories II and III, and constant strain rate tests were not carried out for the unaged material. However, it is shown below that the qualitative behavior in test history I is the same for both the unaged material and groups C and D. Therefore results obtained for aged material may be used to infer the response of the unaged specimens under the same tests conditions. An overview of all tests is given in Table 1.

## RESULTS AND DISCUSSION

### Influence of the Loading Rate at Room Temperature

The stress-strain curves produced by a typical unaged specimen in a series of 8 SRJTs in History I are given in Fig. 2. (Due to the scale the portions of the stress-strain diagrams obtained at the strain rates of  $1.5 \times 10^{-5}$  and  $1.5 \times 10^{-6} \text{ s}^{-1}$  are hardly distinguishable).

It is seen that when material is stressed in the plastic range a unique stress-strain curve is obtained (after a short transient period) for a given strain rate. The material exhibits no strain rate history effect, it "forgets" prior history of strain rate changes: at

any given strain rate material ultimately "returns" to the stress-strain curve characteristic for that particular strain rate. Portions of stress-strain curves obtained at two different strain rates differ ultimately by an approximately constant stress and remain fairly equidistant, which is consistent with earlier studies [20]. An instantaneous linear elastic slope is observed at an instantaneous large (one order of magnitude or more) increase in strain rate, preceded by a relaxation test, at every point in the plastic range. We also observe a negative slope followed by a positive slope as the stress and strain increase at a given strain rate.

No qualitative influence of prior aging on the SRJT response was detected. Stress-strain curves generated by the specimens with different degrees of precipitation were approximately the same. Quantitative effect of aging was observed only for group D and manifested itself in consistently higher flow stresses compared to those reached by the material in other groups. However, the stress differences between the stress-strain curves produced at different strain rates remained essentially unaffected by prior aging.

#### Influence of the Loading Rate at 650 °C

As at room temperature, at 650 °C no significant qualitative effect of prior aging on the rate-dependent material behavior during history I was observed. Specimens with different aging characteristics exhibited qualitatively similar behavior [20]. The quantitative effect of prior aging manifested itself primarily in the absolute values of stress. The highest absolute flow stresses were produced by the material in group D, as was the case at room temperature. The load-strain curves developed for specimens in all aging groups were qualitatively the same. (The peculiarities of the material behavior evident in the load-strain diagrams were obscured in the corresponding stress-strain curves. Hence the load-strain diagrams were used for analysis).

In the discussion of the strain rate sensitivity we will use the load-strain diagrams obtained for specimen 8, group C (Fig. 3). However, all the conclusions made for group C should apply to both the unaged material and the material in group D. The graphs in Fig. 3 demonstrate that:

During the SRJT #1 the monotonic loading segments OA, BC, and DE corresponding to the strain rates of  $1.5 \times 10^{-4} \text{ s}^{-1}$ ,  $1.5 \times 10^{-5} \text{ s}^{-1}$ , and  $1.5 \times 10^{-3} \text{ s}^{-1}$ , respectively, form a smooth continuous curve. No

strain rate sensitivity is observed, even though the strain rate is changed first by one and then by two orders of magnitude.

The influence of the strain rate is first seen in SRJT #1 at pt. F. Here, following a 210 s relaxation test EF and a decrease in strain rate by three orders of magnitude from  $1.5 \times 10^{-3} \text{ s}^{-1}$  to  $1.5 \times 10^{-6} \text{ s}^{-1}$ , the load-strain curve fails to rise to the level established during OA-BC-DE. The load levels produced along FG ( $\dot{\epsilon} = 1.5 \times 10^{-6} \text{ s}^{-1}$ ) are lower than those produced along DE ( $\dot{\epsilon} = 1.5 \times 10^{-3} \text{ s}^{-1}$ ), which is consistent with the conventional idea of the strain rate sensitivity. However, the instantaneous increase of the strain rate by two orders of magnitude at pt. H does not trigger the increase in the load level. The segments FG and HI form a continuous curve. Similar behavior is observed during the SRJT #2. Segments OA, BC, and DE still form a nearly continuous curve, despite the changes in strain rate. However, now one can clearly see the boundaries between these segments, while during the SRJT #1 they were practically indistinguishable up to pt. E. Material response on FG and HI is similar to that during SRJT #1, only now the decrease in the load level between DE and FG is greater than during the SRJT #1.

During the SRJT #3 the strain rate sensitivity becomes noticeable on BC, the load levels on BC are lower than those along OA. However, the increase in strain rate by two orders of magnitude on DE still does not cause the increase in load. Behavior on FG and HI remains nearly unaltered. In all the subsequent SRJTs we observe the same tendencies as in SRJT #3. The load-strain diagrams on BC and DE, and on FG and HI form two continuous curves, the increase by two orders of magnitude in strain rate does not result in any significant change in load. The decreases in strain rate by one order of magnitude between OA and BC, and by three orders of magnitude between DE and FG, however, result in decreases in load levels, which are in keeping with the classic definition of strain rate sensitivity. As the loading in the plastic range progresses, these changes in load levels become more pronounced.

It is seen in Figs. 3a and 3b, that while in general the load level obtained on OA is approximately the same as that reached on HI of the previous SRJT, the load levels reached on OA in SRJTs #4 and 7 are lower than those established on HI of SRJTs #3 and 6, respectively. Such behavior may be due to the cool down and reheating between the SRJTs #3 and 4, and the SRJTs #6 and 7, which was mentioned above.

Test histories II and III were introduced in order to check whether the influence of strain rate, apparent on BC and FG in history I, was due to the preceding relaxation test and/or the rather

low strain rates used on these segments. The load-strain diagrams generated for specimen 10 (group C) in history II (see Fig. 4) show the following:

During the SRJT-1 #1 the strain rate sensitivity first becomes apparent at pt. E. The segments OA, AC, and CE form a smooth continuous curve, despite the changes in strain rate at pts. A and C. The change in strain rate by three orders of magnitude at pt. E results in lower load levels. However, the next strain rate jump at pt. G does not have any noticeable effect on the load-strain diagram, segments EG and GI form a continuous curve. The behavior is akin to that in history I.

During the SRJT-1 #2 the strain rate sensitivity becomes more pronounced: the changes in strain rate result in distinct changes in the load level. (On EG this may be somewhat obscured by the PLC effect, which is discussed later). This trend becomes more marked as the loading progresses from SRJT-1 #2 to failure, the differences between the load levels established on different segments of the test increase. It is noteworthy, that the load-strain diagrams produced along OA and CE form a fairly continuous curve, despite the different strain rates used on these segments. At the same time the load-strain diagram on GI, where the strain rate is the same as on OA, does not form a smooth continuation of the load-strain diagram obtained on OA.

Results of the history III for specimen 13 - group D (shown in Fig. 5) also indicate, that while the strain rate insensitive behavior is observed during the SRJT-2 #1, the influence of the strain rate is evident during the subsequent tests. During the SRJT-2 #1 segments OA, DE, and HI, characterized by different strain rates, form one fairly smooth continuous curve. During the SRJT-2 #2 the strain rate sensitivity becomes more apparent, the three segments of monotonic loading with different strain rates are now distinctly different and could not be merged smoothly. This tendency persists until failure. It should be noted, that even though segments OA and HI, obtained at the same strain rate, form a reasonably continuous curve during the SRJT-2 #3, this is not the case for the SRJT-2 #2.

It is interesting, that while in history II (starting with SRJT-1 #2) the increase (decrease) in strain rate always results in an increase (decrease) in the load level, the increase by an order of magnitude in strain rate on DE in history III triggers the decrease in the load level. This is particularly noticeable in SRJT-2 #2. In order to check whether the material may exhibit negative strain rate sensitivity, the two constant strain rate tensile tests were performed. The corresponding stress-strain curves (see Fig. 6)

demonstrate rate insensitive behavior up to a strain of approximately 6.5%, after which conventional strain rate sensitivity develops (i. e. the higher stresses are produced at the higher strain rate). Thus, the negative strain rate sensitivity, apparent in history III, may be due to the prior history of strain rate changes and relaxation. It has been mentioned that each of the constant strain rate tests was interrupted to readjust the extensometer. For test at  $\dot{\epsilon} = 1.5 \times 10^{-3} \text{ s}^{-1}$ , the interruption time was comparable to the test time (225 s for a 15% strain segment). Thus the discontinuity in the stress-strain curve (a in Fig. 6), where the stresses during the second 15% strain segment start out lower than (but eventually reach) the level established during the first 15% strain interval, may be due to the interruption. In case of the test at  $\dot{\epsilon} = 1.5 \times 10^{-5} \text{ s}^{-1}$  the interruption time was small compared to the test time (22,500 s for a 15% strain interval), and no discontinuities in the stress-strain curve were observed at the points of interruption (b in Fig. 6).

A few remarks common for all specimens tested in histories I-III can be made regarding the presence of the PLC effect. It is clearly seen in Figs. 3-6, that the stress- and load-strain diagrams have a jagged appearance. The serrated flow (PLC effect) is evidently present in all tests. Relationship between the presence of the PLC effect and the strain rate is best demonstrated in Figs. 3 and 4. Serrated flow is most pronounced on the segments of low strain rate (BC and FG in Fig. 3, and AC and EG in Fig. 4), considerably fewer serrations are observed on the high strain rate segments (DE in Fig. 3, and CE in Fig. 4). This tendency is observed at all points in the plastic range. At the same time, we observe that the segments OA and HI (GI in Fig. 4), characterized by  $\dot{\epsilon} = 1.5 \times 10^{-4} \text{ s}^{-1}$ , which are rather densely serrated during the jump tests #1 and 2, exhibit fewer serrations as the straining in the plastic range progresses further.

### Relaxation Behavior at Room Temperature and at 650 °C

Results of the relaxation tests included in History I are summarized in Figs. 7-8 and 9 for room temperature and 650 °C, respectively. In Figs. 7-9 the amounts of stress relaxation produced in 210 s are plotted vs the strain at the beginning of the relaxation test. It is seen that both at room temperature and at 650 °C the amount of relaxation (distances AB, CD, EF, and GH in Fig. 1a) in a given period of time (and therefore the average relaxation rate) is fairly independent of the strain and stress at the beginning of the relaxation test. (Similar behavior was observed in [18, 19]).

Furthermore, the relaxation drop evidently depends on the strain rate preceding the relaxation. This dependence is nonlinear.

It is noteworthy that the short term relaxation is present at 650 °C (as was reported in [2]). One should also note that at 650 °C the relaxation data are somewhat clouded by the PLC effect. Therefore amounts of relaxation plotted in Fig. 9 are generally within  $\pm 5$  MPa (the maximum possible error) of the "real" value. Comparison of relaxation data obtained at 650 °C with that obtained at room temperature demonstrates that the amounts of relaxation increase with temperature. Both room- and elevated-temperature results revealed no qualitative effect of prior aging on relaxation behavior. Some quantitative effect, however, was observed: relaxation drops were somewhat higher for the material with the higher degree of precipitation.

## CONCLUDING REMARKS

### Strain Rate Sensitivity

Room temperature tests demonstrated that the unaged material and the aged specimens with different degrees of precipitation, produce the same qualitative behavior under the SRJTs. When the plastic flow is fully established a unique stress-strain curve is obtained for a given positive strain rate. Material does not exhibit a strain rate history effect. The flow stresses return to the stress-strain curve characteristic for a particular strain rate after initial transients have died out. No qualitative effect of prior aging is observed. The quantitative influence of prior aging manifests itself in increasing flow stresses with an increase in degree of precipitation.

Results of the high-temperature experiments indicate that, unlike at room temperature, at 650 °C the pattern of strain rate sensitivity in SRJT is not set as soon as the plastic flow is fully established, but continues to evolve as the straining in the plastic range progresses. Initially material shows no strain rate sensitivity. At strains greater than 4.5%, a decrease in strain rate by two or three orders of magnitude results in a decrease in flow stresses. The subsequent increase in strain rate by two orders of magnitude, however, does not cause an increase in stress levels. For strains greater than 30%, an increase in strain rate from  $1.5 \times 10^{-6} \text{ s}^{-1}$  to  $1.5 \times 10^{-4} \text{ s}^{-1}$  produces an increase in flow stresses. At the same time, however, a change in strain rate from  $1.5 \times 10^{-5} \text{ s}^{-1}$  to  $1.5 \times 10^{-3} \text{ s}^{-1}$  does not cause a discontinuity in the stress-strain curve.

Material response in history III (conducted at 650 °C) shows that the rate sensitivity is influenced by the presence of relaxation tests. When the relaxation periods are omitted, for strains greater than 6.45% an increase (decrease) in strain rate results in a distinct increase (decrease) in flow stresses. In none of the histories I, II, or III, do we observe a unique stress-strain curve established for a given strain rate. Together with the dependence of the rate sensitivity pattern on the presence of relaxation tests this indicates that the material exhibits a strain rate history effect at 650 °C. Further testing, however, would be necessary to reach a more definite conclusion. At 650 °C prior aging had no noticeable effect on the strain rate sensitivity behavior in a qualitative sense.

### Relaxation Behavior

Test results revealed no significant qualitative effect of temperature on the relaxation behavior. Both at room temperature and at 650 °C, the stabilized amount of relaxation in a certain period of time is independent of the stress and strain at the beginning of relaxation, but depends nonlinearly on the strain rate preceding the relaxation test. A marked quantitative effect of temperature on relaxation was observed: amounts of relaxation at 650 °C were considerably larger than those at room temperature. Prior aging had apparently no qualitative effect on the relaxation behavior at either room temperature or at 650 °C. However, some quantitative influence was observed: specimens with the higher degree of precipitation produced higher amounts of relaxation.

### ACKNOWLEDGEMENT

Department of Energy donated the test material and supported this study. E. J. Tracey of General Electric Company performed the heat treatment of specimens.

### DISCLAIMER

This report was prepared as an account of work sponsored by an agency of the United States Government. Neither the United States Government nor any agency thereof, nor any of their employees, makes any warranty, express or implied, or assumes any legal liability or responsibility for the accuracy, completeness, or usefulness of any information, apparatus, product, or process disclosed, or represents that its use would not infringe privately owned rights. Reference herein to any specific commercial product, process, or service by trade name, trademark, manufacturer, or otherwise does not necessarily constitute or imply its endorsement, recommendation, or favoring by the United States Government or any agency thereof. The views and opinions of authors expressed herein do not necessarily state or reflect those of the United States Government or any agency thereof.

## REFERENCES

1. Krempl, E., "On the Interaction of Rate and History Dependence in Structural Metals", Acta Mechanica, 22, 1975, pp. 53-90.
2. Nouailhas, D., "A Viscoplastic Modeling Applied to Stainless Steel Behavior", Constitutive Laws for Engineering Materials. Theory and Applications, vol. 1, Desai, C. S., Krempl, E., Kiousis, P. D., and Kundu, T., Eds., Proceedings of the Second International conference on Constitutive laws for Engineering Materials: Theory and Applications, Elsevier, New York, 1987, pp. 717-724.
3. Goodall, I. W., Hales, R., and Walters, D. J., "On constitutive Relations and Failure Criteria of an Austenitic Steel under Cyclic Loading at Elevated Temperature", IUTAM Symposium, Leicester, CEBG Report RB/B/N 4916, 1980.
4. Clement, G., Guionnet, C., "Analysis of Biaxial Experiments on 316 Steels at Elevated Temperature", Transactions of the 8th International Conference on Structural Mechanics in Reactor Technology, vol. L, 1985, pp. 43-48.
5. Inoue, T., Imatani, S., Sahashi, T., "Some Remarks on the Inelastic Behavior of High Temperature Materials under Biaxial Stress State", Transactions of the 8th International Conference on Structural Mechanics in Reactor Technology, vol. L, 1985, pp. 7-14.
6. Penning, P., "Mathematics of the Portevin-LeChatelier Effect", Acta Metallurgica, vol. 20, 1972, pp. 1169-1175.
7. Wijler, A., and Schade van Westrum, J., "Serrated Yielding and Inhomogeneous Deformation in Au(14at%Cu)", Scripta Metallurgica, vol. 5, 1971, pp. 159-164.
8. Blakemore, J. S., "The Portevin-LeChatelier Effect in Carburized Nickel Alloys", Metallurgical Transactions, vol.1, 1970, pp. 1281-1285.
9. Van den Brink, S. H., van den Beukel, A., and McCormick, P. G., "Strain Rate Sensitivity and the Portevin-LeChatelier Effect in Au-Cu Alloys", Physica Status Solidi, (a) 30, 1975, pp. 469-477.
10. McCormick, P. G., "the Portevin-LeChatelier Effect in a Pressurized Low Carbon Steel", Acta Metallurgica, vol. 21, 1973, pp. 873-878.
11. Jenkins, C. F., and Smith, G. V., "Serrated Plastic Flow in Austenitic Stainless Steel", Transactions of the Metallurgical Society of AIME, vol. 245, 1969, pp. 2149-2156.

12. Wycliffe, P., Kocks, U. F., and Embury, J. D., "On Dynamic and Static Strain Aging in Substitutional and Interstitial Alloys", Scripta Metallurgica, vol. 14, 1980, pp. 1349-1354.

13. Coffin, L. F., "The Effect of Quench Aging and Cyclic-Strain Aging on Low Carbon Steel", Transactions of ASME, Journal of Basic Engineering, 87D, 1965, pp. 351-362.

14. Van den Beukel, A., and Kocks, U. F., "The Strain Dependence of Static and Dynamic Strain-Aging", Acta Metallurgica, vol. 30, 1982, pp. 1027-1034.

15. Van den Beukel, A., "Theory of the Effect of Dynamic Strain Aging on Mechanical Properties", Physica Status Solidi, (a) 30, 1975, pp. 197-206.

16. Krempl, E., "The Role of Servocontrolled Testing in the Development of the Theory of Viscoplasticity Based on Total Strain and Overstress", Mechanical Testing for Deformation Model Development, ASTM STP 765, Rohde, R. W., and Swearingen, J. C., Eds., ASTM, 1982, pp. 5-28.

17. Krempl, E., "An Experimental Study of Room-Temperature Rate-Sensitivity, Creep and Relaxation of AISI Type 304 Stainless Steel", Journal of the Mechanics and Physics of Solids, vol. 27, 1979, pp. 363-375.

18. Kujawski, D., Kallianpur, V., and Krempl, E., "An Experimental Study of Uniaxial Creep, Cyclic Creep and Relaxation of AISI Type 304 Stainless Steel at Room Temperature", Journal of the Mechanics and Physics of Solids, vol. 28, 1980, pp. 129-148.

19. Kujawski, D., and Krempl, E., "The Rate (Time) - Dependent Behavior of Ti-7Al-2Cb-1Ta Titanium Alloy at Room Temperature under Quasi-Static Monotonic and Cyclic Loading", Journal of Applied Mechanics, vol. 103, No. 1, 1981, pp. 55-63.

20. Ruggles, M. B., Ph. D. Thesis, Rensselaer Polytechnic Institute, Troy, New York, 1987.

TABLE 1.

Summary of Tests Performed.

Specimen #	Age Group	Test History	Temperature (°C)
1	Unaged	I	20
2	"	I	20
3	"	I	20
4	C	I	20
5	D	I	20
6	Unaged	I	650
7	C	I	650
8	C	I	650
9	D	I	650
10	C	II	650
11	C	III	650
12	C	III	650
13	D	III	650
14	C	*	650
15	D	*	650
16	D	**	650

\*  $\dot{\epsilon} = 1.5 \times 10^{-3} \text{ s}^{-1} = \text{const}$

\*\*  $\dot{\epsilon} = 1.5 \times 10^{-5} \text{ s}^{-1} = \text{const}$

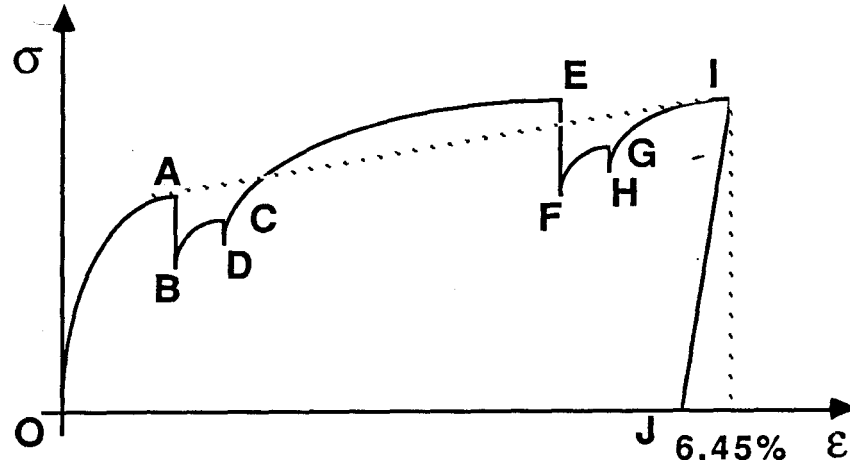


Figure 1a. Strain rate jump test (SRJT).

---

Strain Rate Jump Test Characteristics

---

Segment	Time (s)	Strain Accumulation (%)	Strain Rate (s <sup>-1</sup> )
OA	100	1.50	$1.5 \times 10^{-4}$
AB	210	Relaxation	Relaxation
BC	100	0.15	$1.5 \times 10^{-5}$
CD	210	Relaxation	Relaxation
DE	20	3.00	$1.5 \times 10^{-3}$
EF	210	Relaxation	Relaxation
FG	2100	0.30	$1.5 \times 10^{-6}$
GH	210	Relaxation	Relaxation
HI	100	1.50	$1.5 \times 10^{-4}$

---

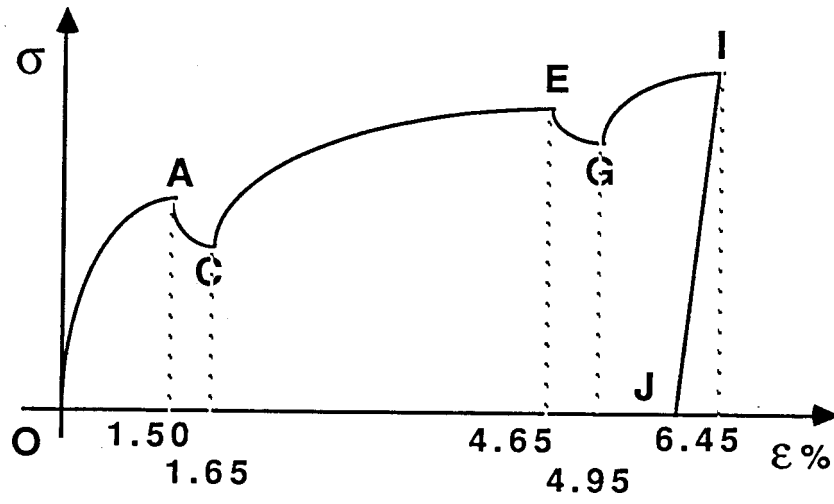


Figure 1b. SRJT-1.

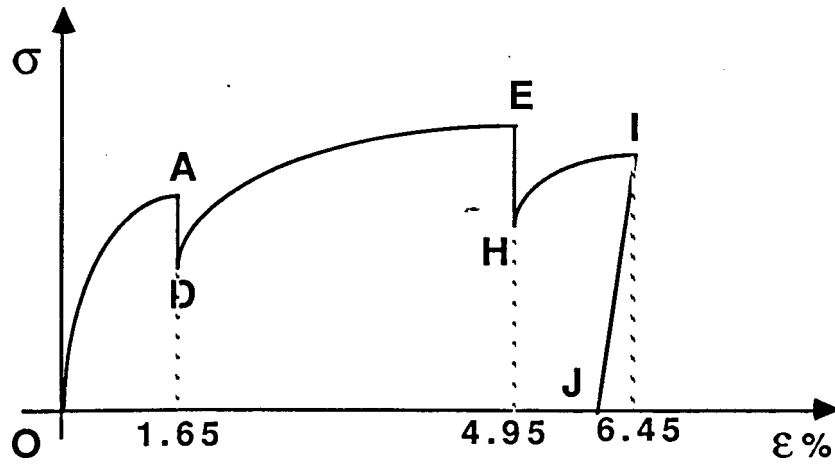


Figure 1c. SRJT-2.

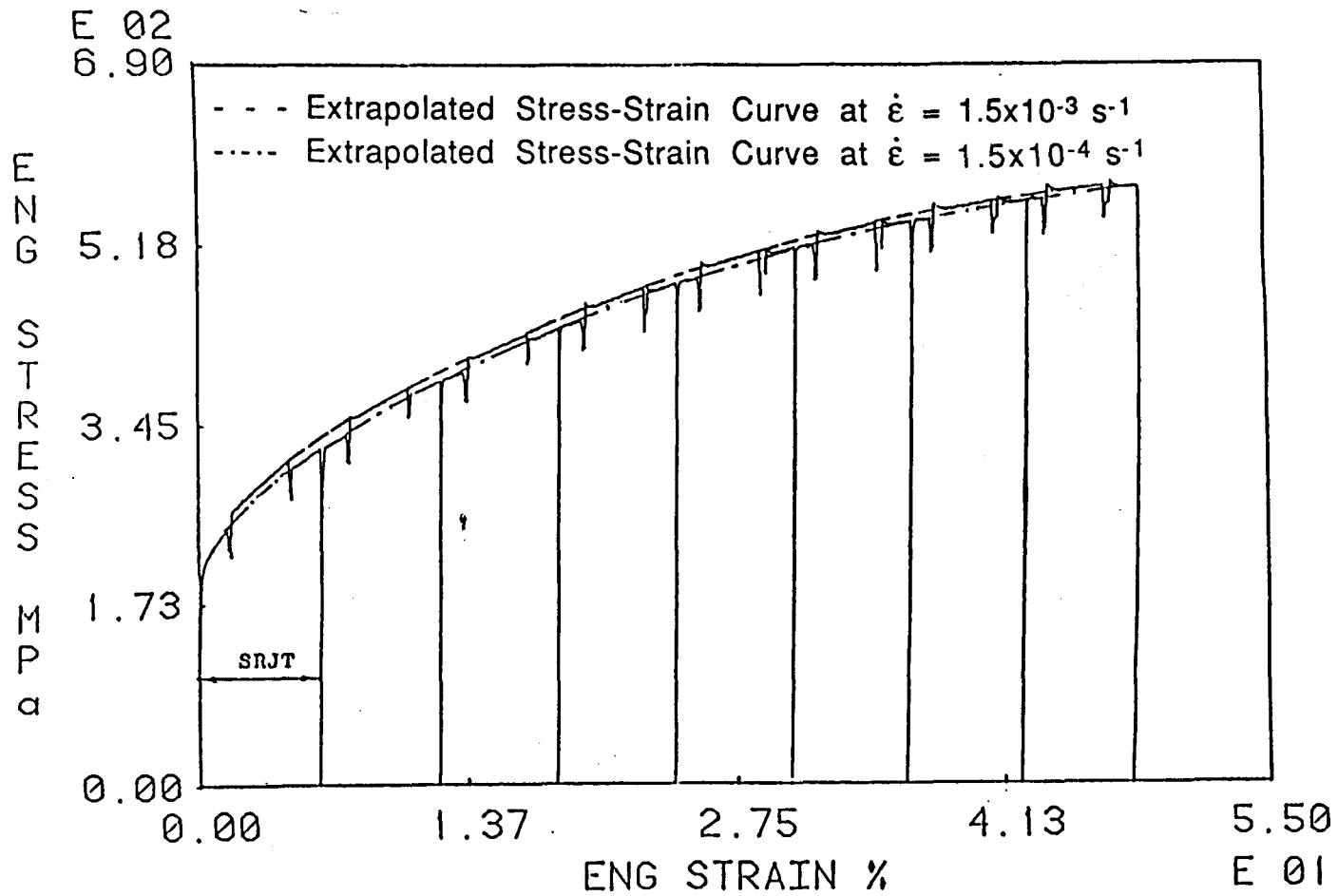


Figure 2.  
 Room Temperature. Test History I. Unaged Material. Specimen # 2.  
 Stress-Strain Curves.

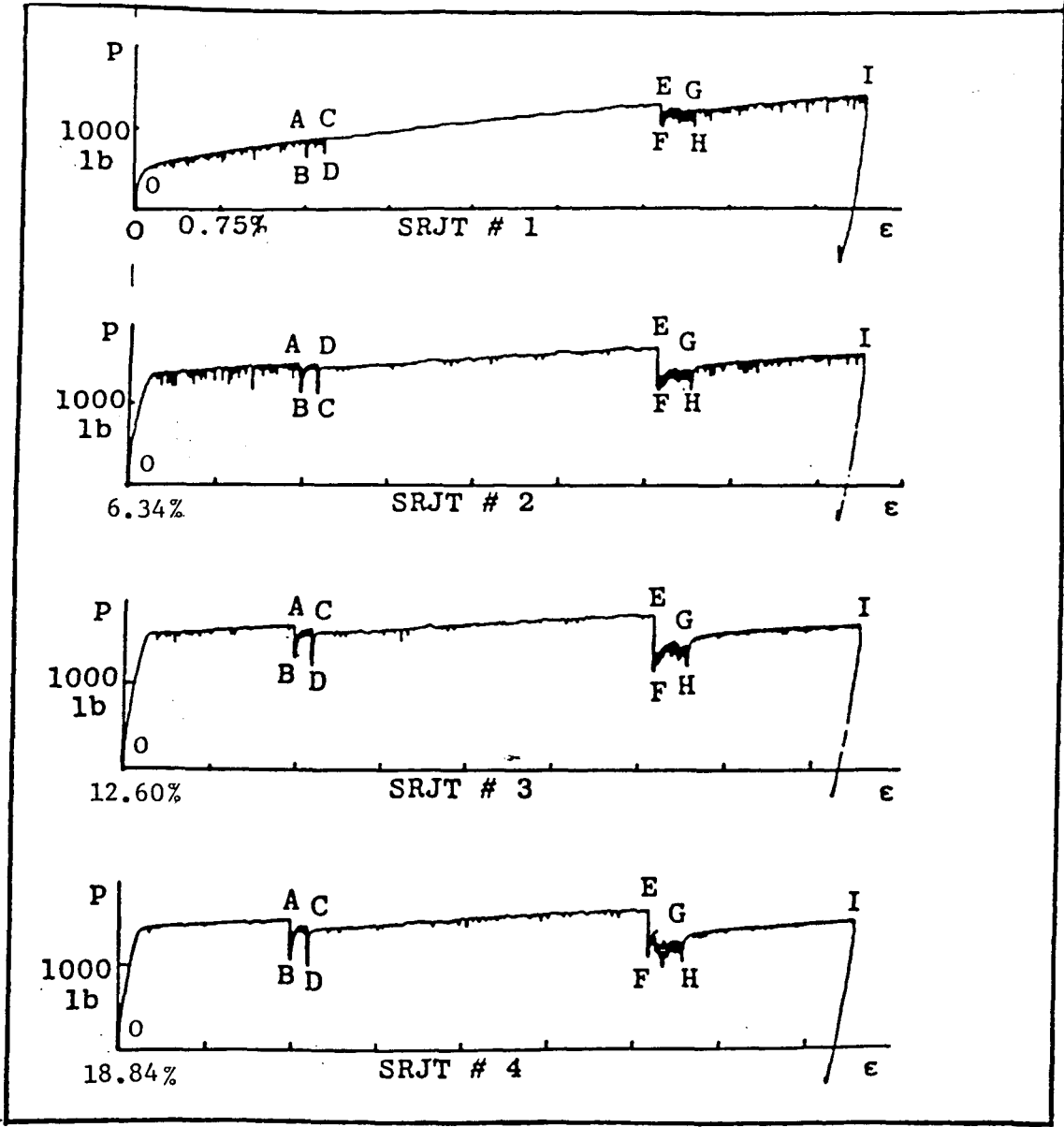


Figure 3a.  
T=650° C. Test History I. SRJT #1-4. Group C. Specimen # 8.  
Load P vs Strain  $\epsilon$ . (Cross-Sectional Area in the Gage Section  
= 0.04975 in<sup>2</sup>).

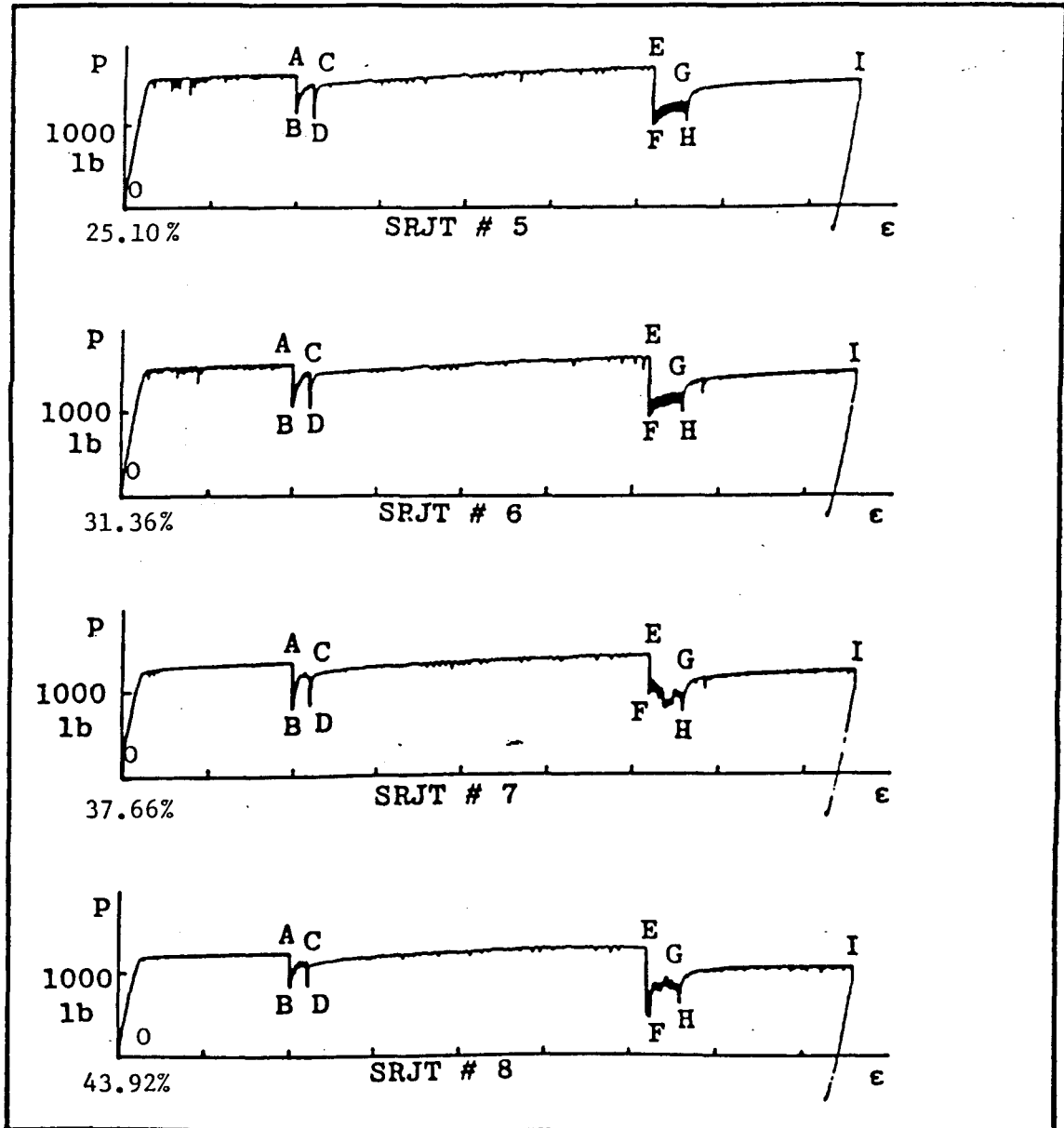


Figure 3b.  
 T=650° C. Test History I. SRJT # 5-8. Group C. Specimen # 8.  
 Load P vs Strain  $\epsilon$ . (Cross-Sectional Area in the Gage Section  
 = 0.04975 in<sup>2</sup>).

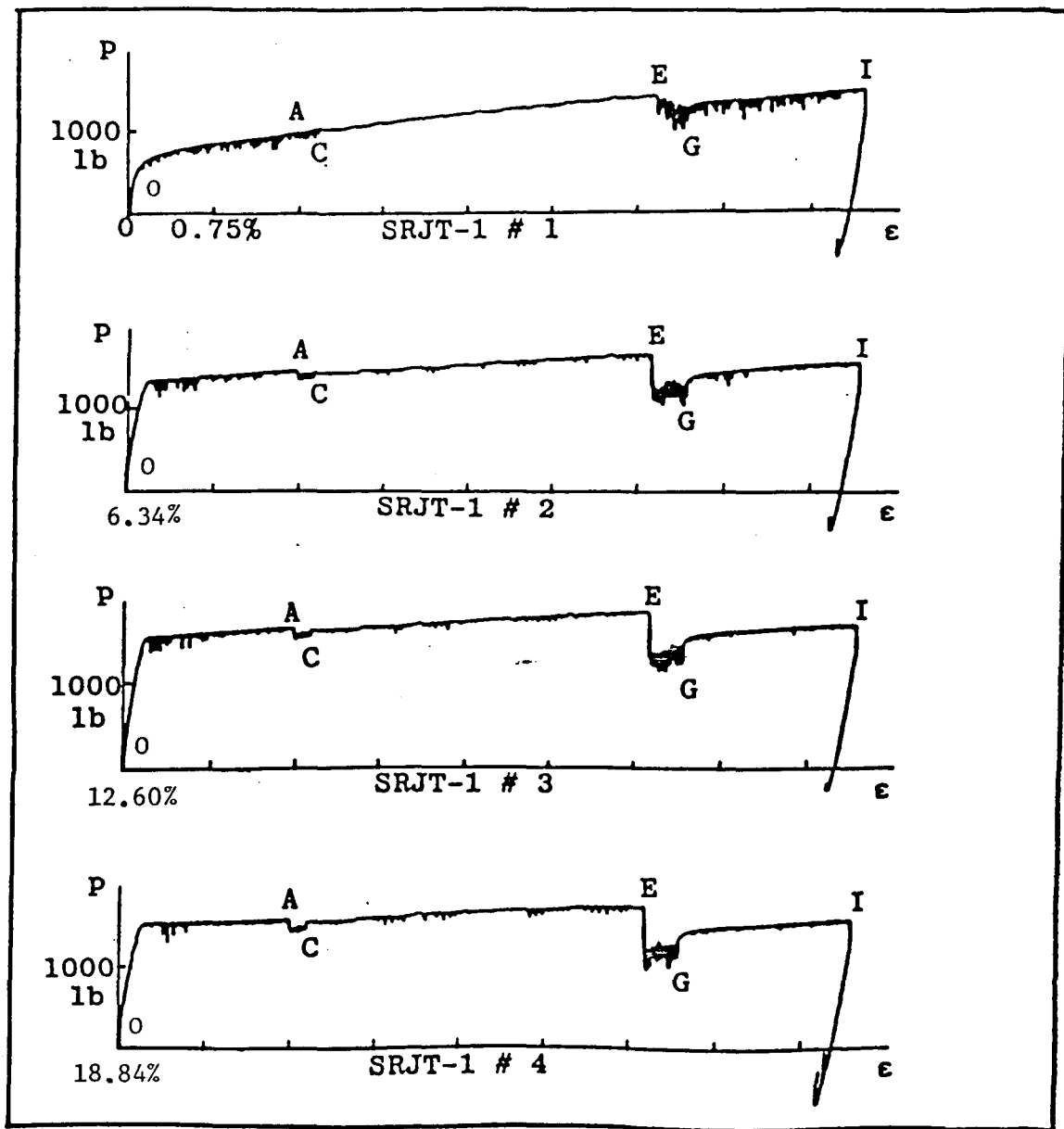


Figure 4a.  
 T=650° C. Test History II. SRJT-1 # 1-4. Group C. Specimen # 10.  
 Load P vs Strain  $\epsilon$ . (Cross-Sectional Area in the Gage Section  
 = 0.04857 in<sup>2</sup>).

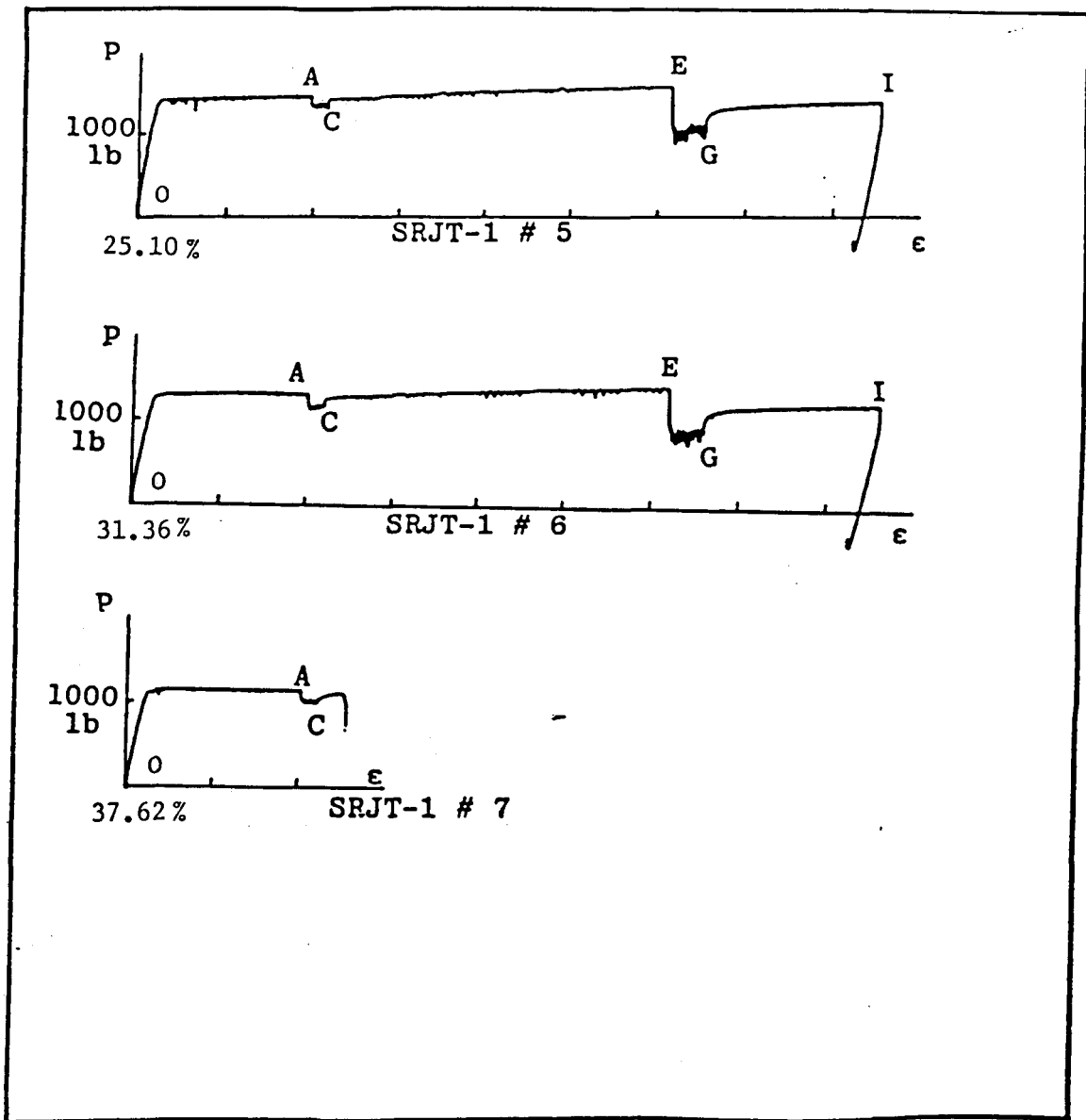


Figure 4b.

T=650° C. Test History II. SRJT-1 # 5-7. Group C. Specimen # 10.  
Load P vs Strain  $\epsilon$ . (Cross-Sectional Area in the Gage Section  
= 0.04857 in<sup>2</sup>).

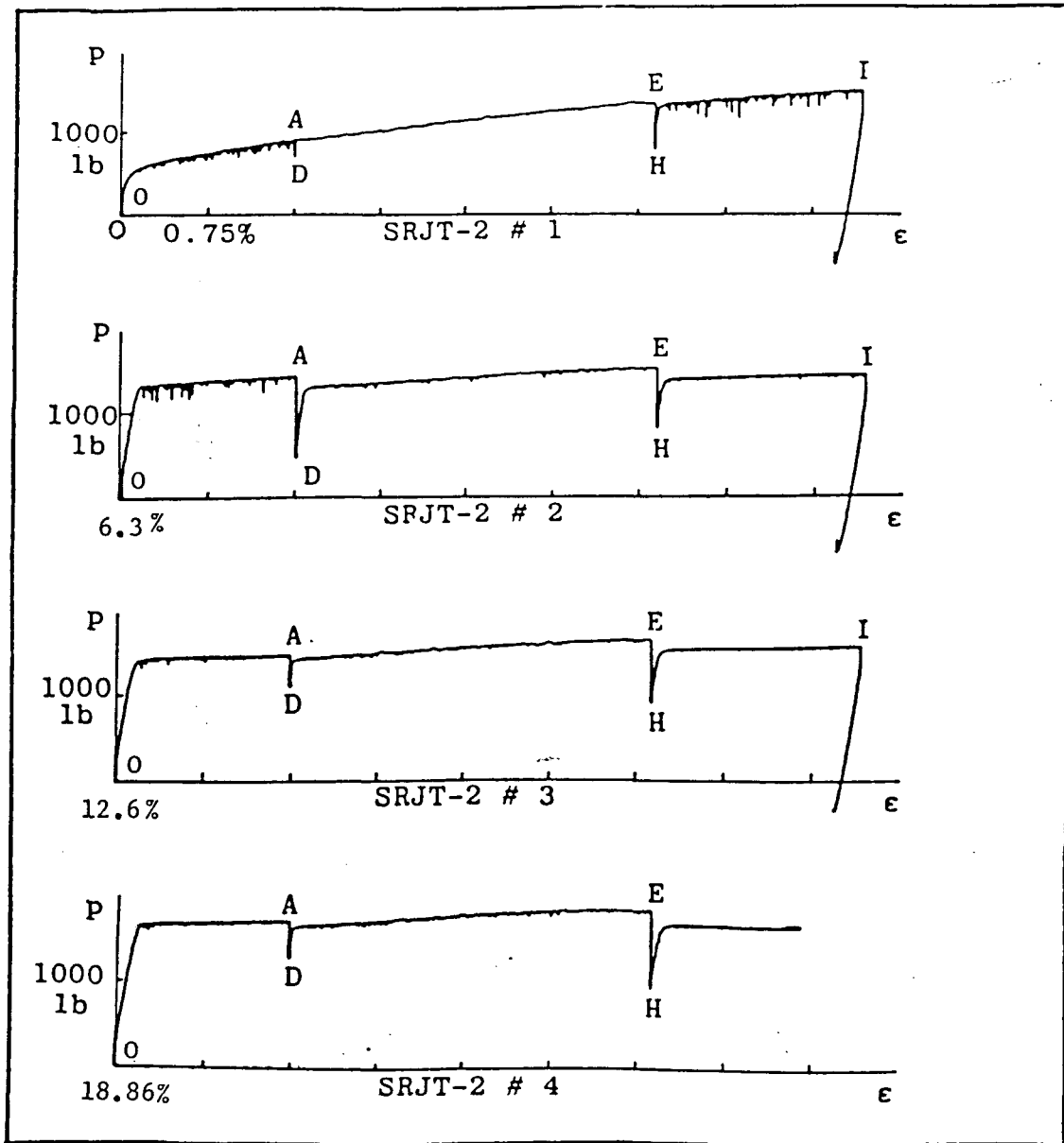


Figure 5.  
 $T=650^{\circ} C$ . Test History III. SRJT-2 # 1-4. Group D. Specimen # 13.  
 Load P vs Strain  $\epsilon$ . (Cross-Sectional Area in the Gage Section  
 $= 0.04896 \text{ in}^2$ ).

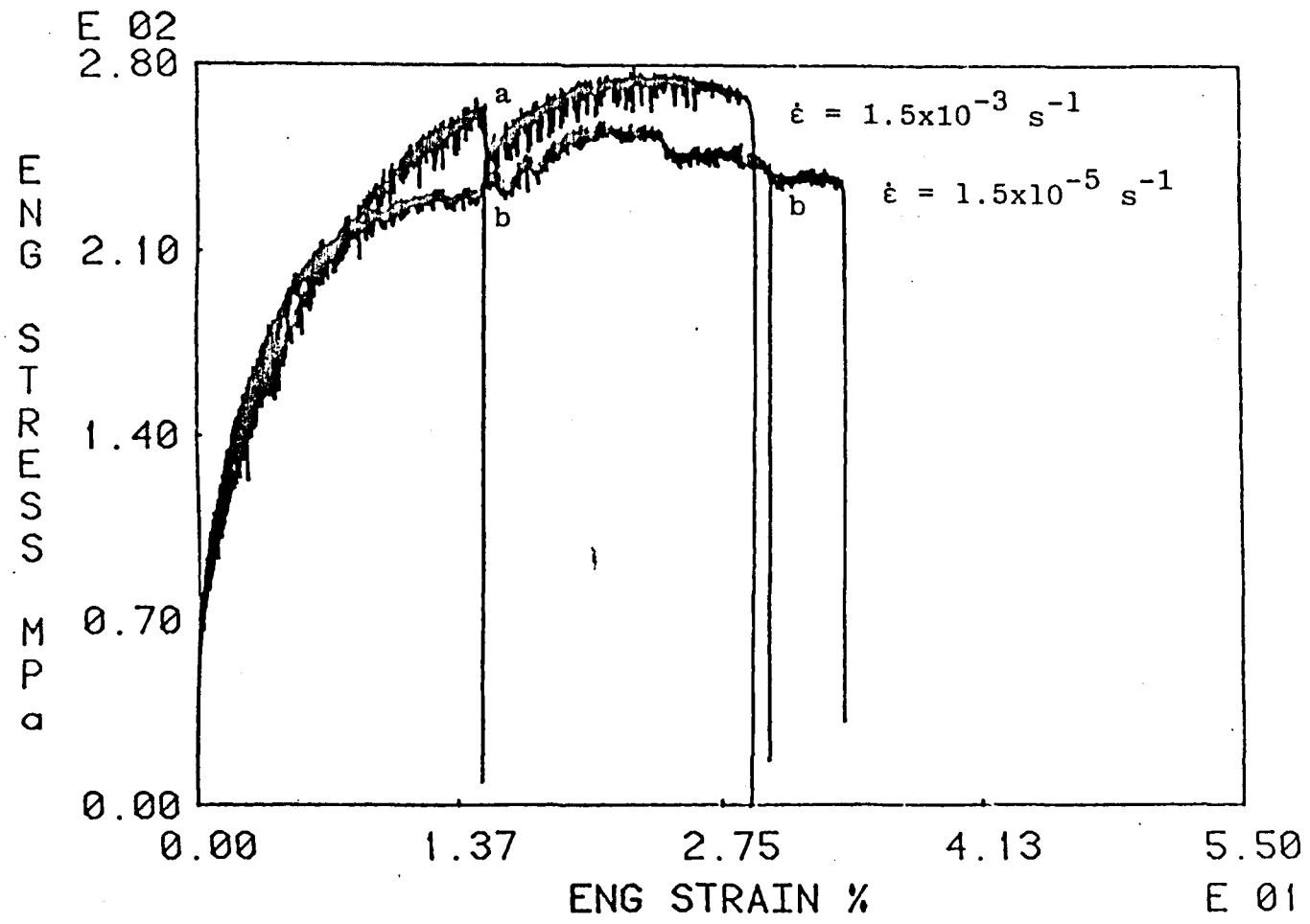


Figure 6.  
 T=650° C. Constant Strain Rate Tests. Stress-Strain Curves.  
 Specimen # 15, Group D,  $\dot{\epsilon} = 1.5 \times 10^{-3} \text{ s}^{-1}$ .  
 Specimen # 16, Group D,  $\dot{\epsilon} = 1.5 \times 10^{-5} \text{ s}^{-1}$ .

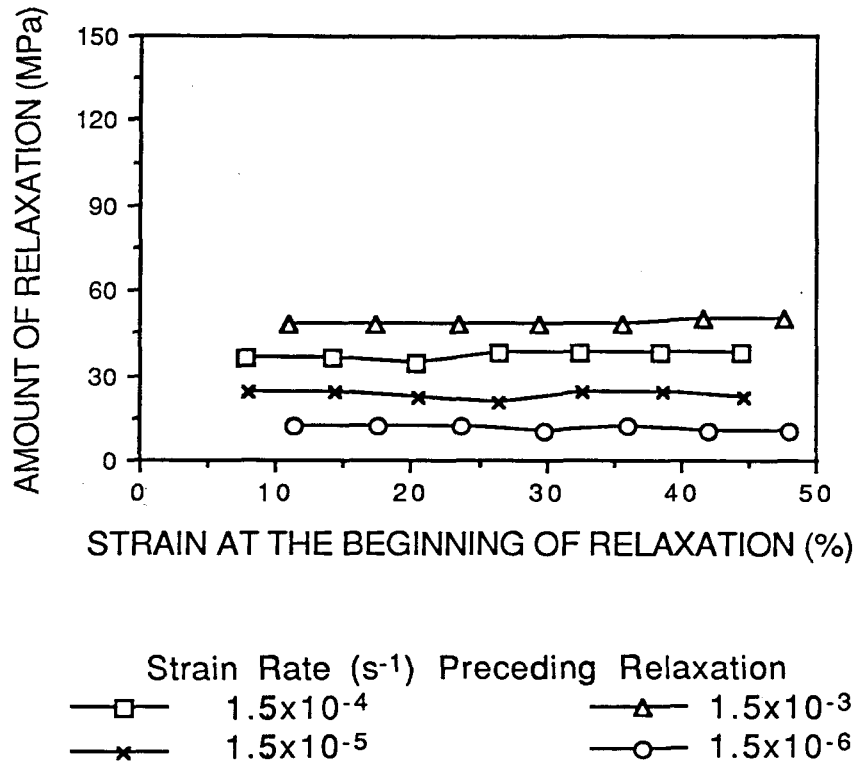


Figure 7. Room temperature. Test history I. Unaged material. Amount of relaxation in 210 s vs strain at the beginning of relaxation.

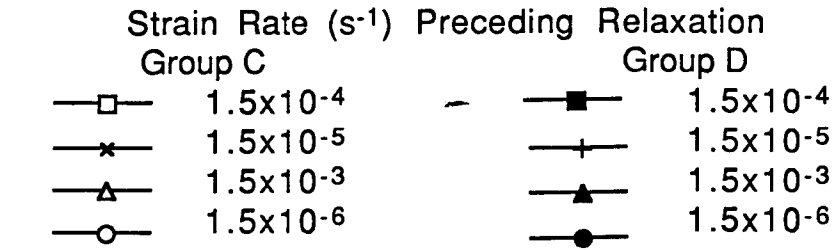
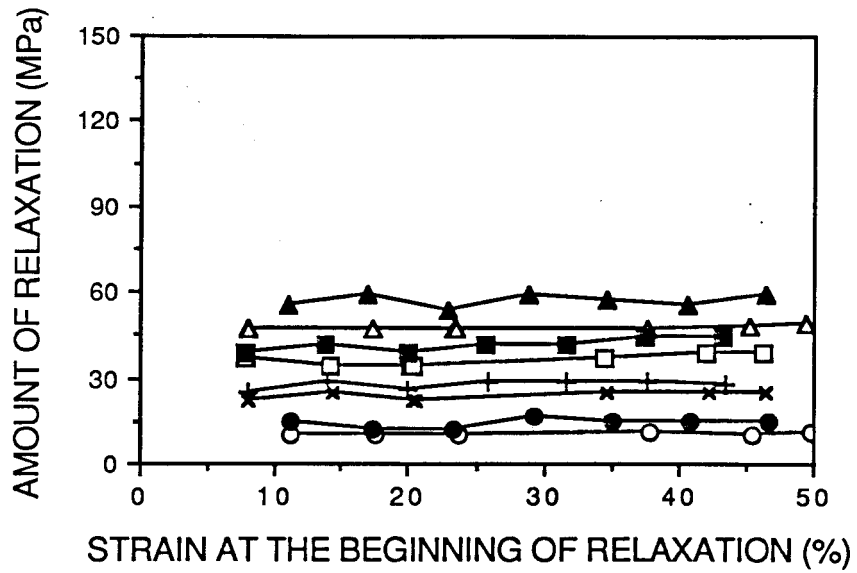


Figure 8. Room temperature. Test history I. Aged material. Amount of relaxation in 210 s vs strain at the beginning of relaxation.

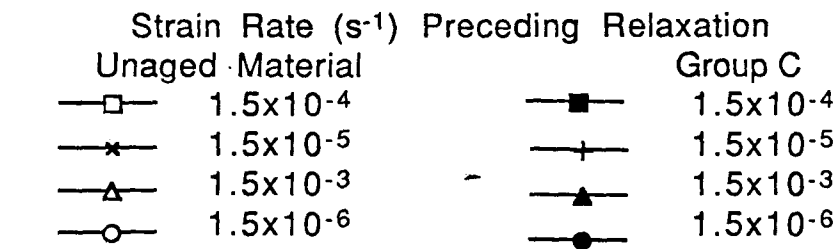
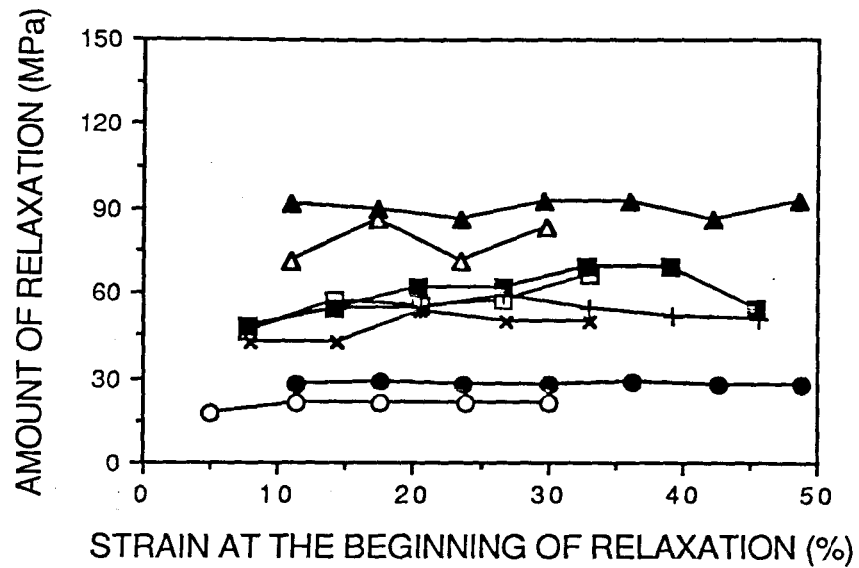


Figure 9. T=650 °C. Test history I. Amount of relaxation in 210 s vs Strain at the beginning of relaxation.